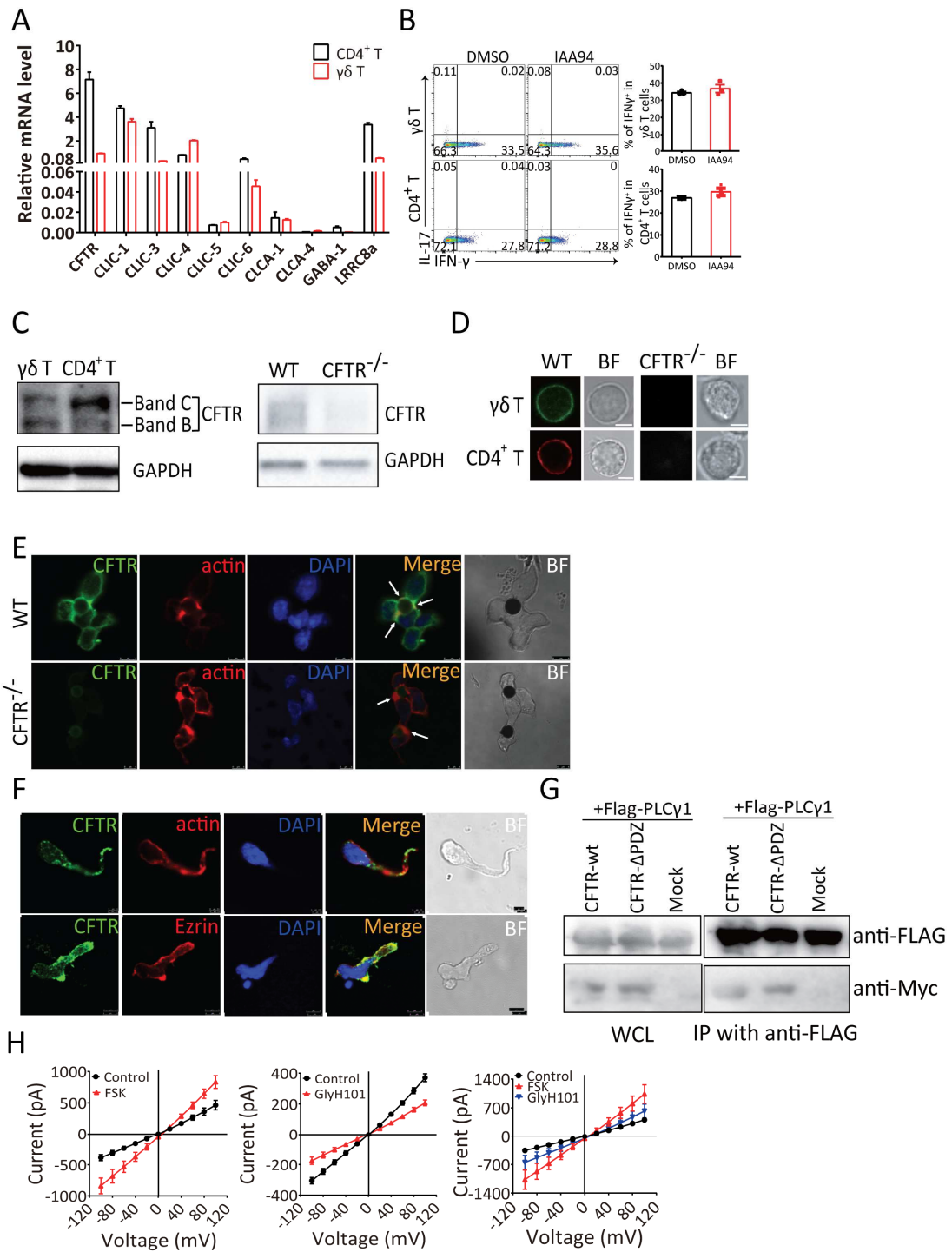


Supplementary Information for

**CFTR is a negative regulator of  $\gamma\delta$  T cell IFN- $\gamma$  production and anti-tumor immunity.**

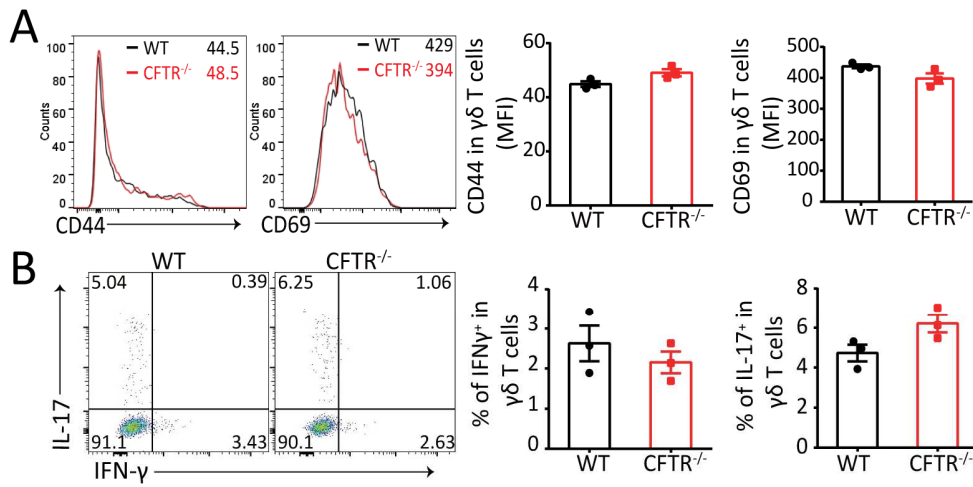
Duan et al.



Duan et al. Fig.S1

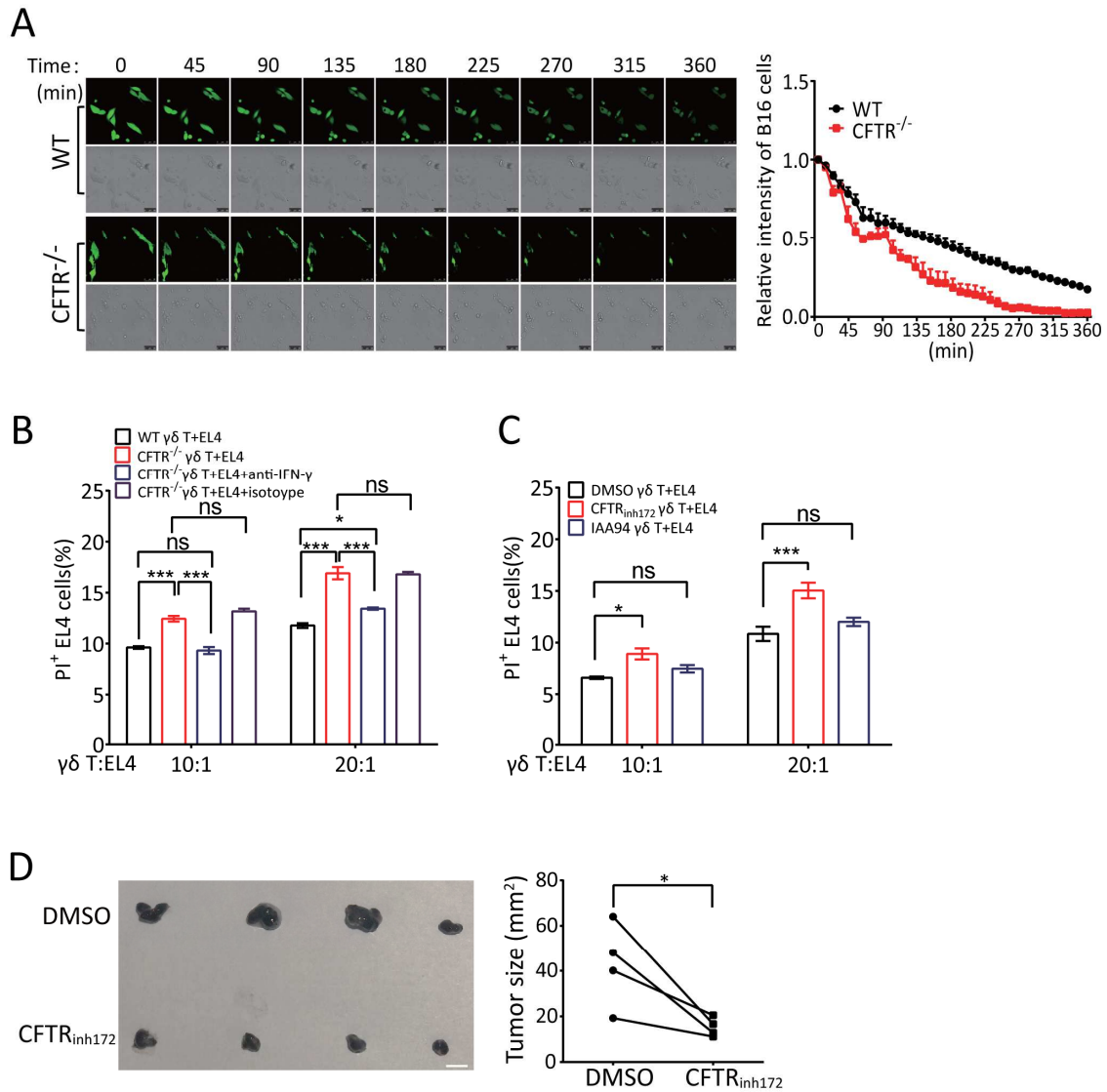
**Fig S1. CFTR was highly expressed in the cell surface of  $\gamma\delta$  T and  $CD4^+$  T cells, and CFTR polarized towards to immunological synapse via cytoskeleton in  $\gamma\delta$  T cells.** A) Quantitative PCR analysis of different types of chloride ion channels in splenic  $CD4^+$  and  $\gamma\delta$  T cells (n=3); B) Flow cytometry of splenic  $\gamma\delta$  T/ $CD4^+$  T cells with PMA (50 ng/ml) and ionomycin (1  $\mu$ g/ml) stimulation for 6 h in the presence of CLICs inhibitor IAA94 (50  $\mu$ M) or its vehicle DMSO to detect IFN- $\gamma$  and IL-17 production (n=3); C) Left: Immunoblot analysis of CFTR expression in mouse splenic  $\gamma\delta$  and  $CD4^+$  T cells on the 10% SDS-PAGE gel. Doublets at ~140 kDa and ~180 kDa correspond to the nonglycosylated and glycosylated forms of CFTR. GAPDH was detected as loading control; Right: Immunoblot analysis of CFTR expression in mouse splenic WT and CFTR<sup>-/-</sup>  $\gamma\delta$  T cells on the 10% SDS-PAGE gel; D) Confocal microscopy of the expression of CFTR in splenic WT or CFTR<sup>-/-</sup>  $CD4^+$  and  $\gamma\delta$  T cells stained with Alexa Fluor 488-conjugated anti-mouse IgG ( $\gamma\delta$  T) or mouse anti-CFTR followed by Alexa Fluor 594-conjugated anti-mouse IgG ( $CD4^+$  T) (scale bar: 2.5  $\mu$ m); E) Confocal microscopy of the stimulated WT or CFTR<sup>-/-</sup>  $\gamma\delta$  T cells with Dynabeads® Mouse T-Activator CD3/CD28, and stained with mouse anti-CFTR antibody followed by Alexa Fluor 488-conjugated anti-mouse IgG, and with Alexa Fluor 594-conjugated phalloidin (arrowheads indicate the immunosynapse area) (scale bar: 5  $\mu$ m); F) Confocal microscopy of the stimulated  $\gamma\delta$  T cells with Dynabeads® Mouse T-Activator CD3/CD28, and stained with mouse anti-CFTR followed by Alexa Fluor 488-conjugated anti-mouse IgG, and with Alexa Fluor 594-conjugated phalloidin or with rabbit anti-ezrin followed by Alexa Fluor 594-conjugated anti-rabbit IgG (scale bar: 5  $\mu$ m); G) Immunoblot analysis of HEK293T cells transfected with Flag-tagged PLC $\gamma$ -1 and Myc-tagged CFTR-wt, Myc-tagged CFTR- $\Delta$ PDZ, or Myc empty vector (Mock). Cells were immunoprecipitated with anti-FLAG M2 magnetic beads and probed with anti-Myc or anti-Flag antibodies. Data are representative of at least three experiments; H) Current-voltage relationship of the Forskolin (FSK, 10  $\mu$ M)-induced current (P=0.002, n=7) (left) and the GlyH101(10  $\mu$ M)-inhibited current (P=0.002, n=7)

(middle), and inhibition by GlyH101 to FSK-induced current (FSK:  $P=0.042$ , GlyH101:  $P=0.007$ ,  $n=5$ ) in  $\gamma\delta$  T cells.



Duan et al. Fig.S2

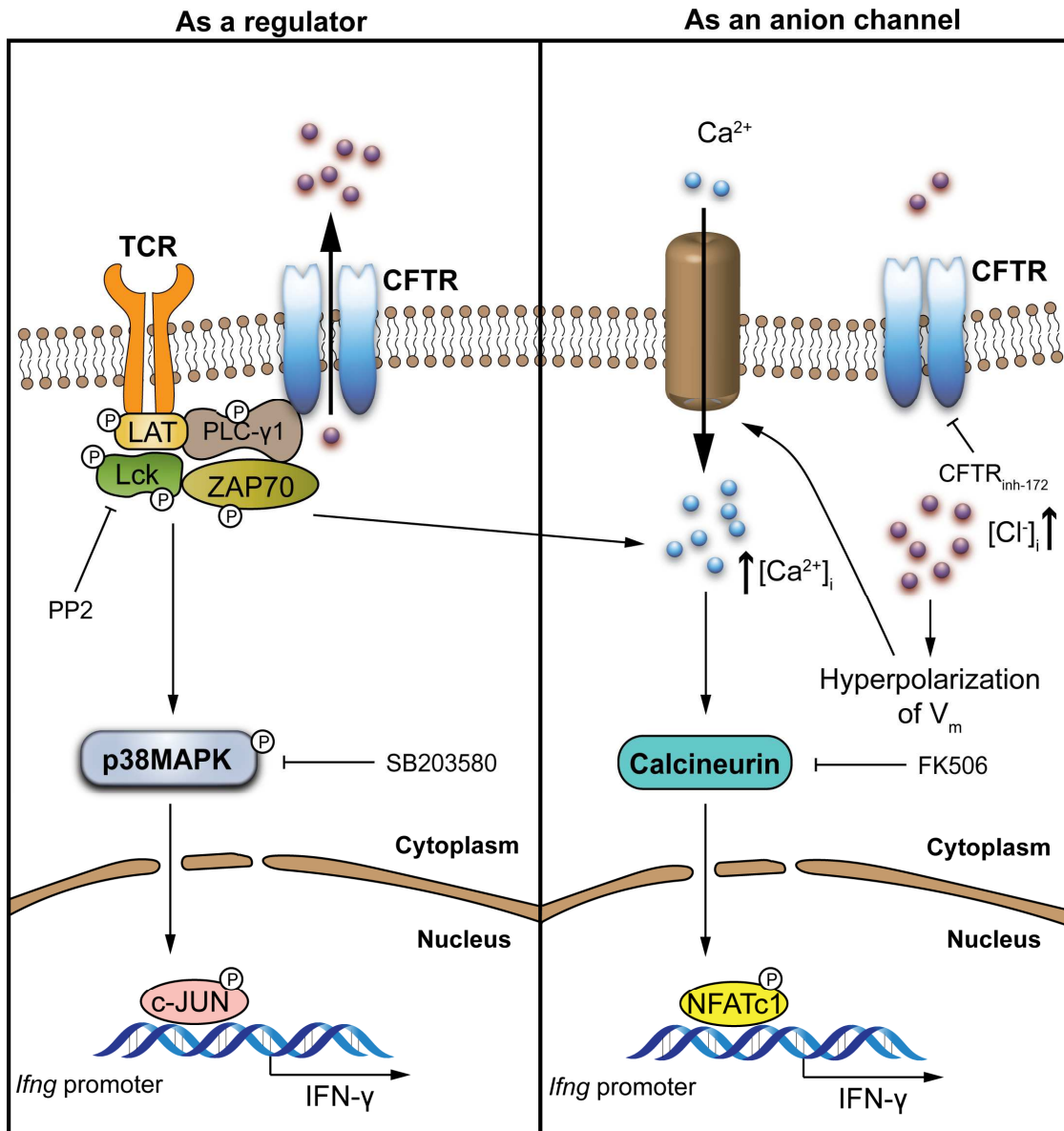
**Fig S2. CFTR exerted no effect on the thymic programming.** A) representative flow cytometry and statistical analysis of CD44 and CD69 in WT or CFTR<sup>-/-</sup> thymic γδ T cells (n=3). B) representative flow cytometry and statistical analysis of WT or CFTR<sup>-/-</sup> thymic γδ T cells with the PMA (50 ng/ml) and ionomycin (1 μg/ml) stimulation for 6 h to detect the IFN-γ and IL-17 production (n=3).



Duan et al. Fig.S3

**Fig S3. CFTR deficiency and dysfunction in  $\gamma\delta$  T cells displayed higher killing ability against B16 melanoma and EL4 lymphoma.** A) The real-time confocal microscopy and statistical analysis of coculture of the in vitro-expanded WT or CFTR<sup>-/-</sup>  $\gamma\delta$  T cells with calcein AM-labeled B16 cells in 5:1 ratio for 6 h (n=5); B) Co-culture of the in vitro-expanded WT or CFTR<sup>-/-</sup>  $\gamma\delta$  T cells with CFSE labeled EL4 cells in indicated ratio, anti-IFN- $\gamma$  (10  $\mu$ g/ml ) was added to neutralize the cytotoxicity and isotype control antibody was added. 6 h later, dead EL4 cells were assessed by PI staining (\*\*\*, p<0.001; \*, p<0.05; ns, not significant; n=3); C)

*In vitro*-expanded  $\gamma\delta$  T cells were pretreated with CFTR inhibitor CFTR<sub>inh172</sub> (5  $\mu$ M), CLICs inhibitor IAA94 (50  $\mu$ M) or its vehicle DMSO for 2 h, and then co-cultured with CFSE labeled EL4 cells in indicated ratio. 6 h later, the dead EL4 cells were assessed by PI staining (\*\*\*,  $p < 0.001$ ; \*,  $p < 0.05$ ; ns, not significant;  $n = 3$ ); D) B16 cells ( $2 \times 10^5$  cells/mouse) were mixed with *in vitro*-expanded and purified WT or CFTR<sub>inh172</sub><sup>-</sup> treated  $\gamma\delta$  T cells ( $0.5 \times 10^5$  cells/mouse) and s.c. injected into B6 TCR  $\delta^{-/-}$  mice ( $n = 4$  per each group). At day 12 post tumor injection, tumors were isolated (left panel, scale bar=5mm) and tumor sizes were measured (right panel, paired t test; \*,  $p < 0.05$ ).



Duan et al. Fig.S4

**Fig S4. Proposed model for regulating IFN- $\gamma$  production in  $\gamma\delta$  T cells.** We observed that molecular mechanisms underlie the regulation of CFTR on IFN- $\gamma$  production by  $\gamma\delta$  T cells were either TCR dependent or Ca<sup>2+</sup> influx in  $\gamma\delta$  T cells. In one hand, CFTR, which was served as a part of TCR signaling cascade and a regulator, suppresses Lck-P38-c-Jun pathway as well as TCR-stimulated Ca<sup>2+</sup> influx and decreases IFN- $\gamma$  expression. On the other hand, CFTR functions as a chloride channel via TCR-independent manner. Once CFTR channel activity is



blocked, the resultant elevated  $[Cl^-]_i$  hyperpolarizes  $V_m$  and triggers  $Ca^{2+}$  influx, which in turn leads to downstream Calcineurin-NFATc1 signaling pathway and IFN- $\gamma$  production of  $\gamma\delta$  T cells. Proper inactivation of CFTR could enhance anti-tumor immunity in  $\gamma\delta$  T cell-mediated cancer immunotherapy.